Reversal of magnetic field rotation in the reconnection layer due to shear flow effects

Xiaoxia Sun,[1,2] Yu Lin,[2,3] and Xiaogang Wang[1,2]

Received 22 April 2006; revised 15 August 2006; accepted 30 August 2006; published 9 November 2006.

[1] We investigate the effects of shear flows on the so-called "component reconnection," in which the guide field $B_y \neq 0$, by solving a one-dimensional Riemann problem for magnetopause reconnection using a resistive MHD simulation. Specifically, we consider the existence of a shear flow perpendicular to the antiparallel magnetic field B_z, while a finite shear flow tangential to B_z may also be present. In the cases without a magnetosheath flow and having thus a sheared flow across the reconnection layer, two time-dependent intermediate shocks TDIS and TDIS′ are present on the magnetosheath side and the magnetospheric side, respectively, and the strength of TDIS is much stronger than that of TDIS′. Nevertheless, the existence of the shear flows modifies the structure and strength of the time-dependent intermediate shocks significantly. (1) The perpendicular shear flow V_{y0} can lead to the reversal of the rotation sense of the tangential magnetic field in time-dependent intermediate shocks. The critical shear flow speeds, V_c and V'_c, for the reversal of field rotations in TDIS and TDIS′, respectively, are calculated. (2) For shear flow speed $V_{y0} = V_c$, the strong TDIS is replaced by a steady intermediate shock (IS), whereas at $V_{y0} = V'_c$ an Alfvén wave pulse is present in the reconnection layer. (3) The presence of tangential shear flow V_{z0} alters not only the strength of TDIS and TDIS′ but also the critical speeds V_c and V'_c. The critical shear flow speeds obtained from our simulation are found to agree very well with those from the ideal magnetohydrodynamics (MHD), in which the time-dependent intermediate shocks are replaced by rotational discontinuities.

Citation: Sun, X., Y. Lin, and X. Wang (2006), Reversal of magnetic field rotation in the reconnection layer due to shear flow effects, *J. Geophys. Res.*, *111*, A11210, doi:10.1029/2006JA011812.

1. Introduction

[2] Magnetohydrodynamic (MHD) theories [*Heyn et al.*, 1988; *Petschek*, 1964] predict that in the outflow region of magnetic reconnection, i.e., the reconnection layer, there may exist various MHD discontinuities, including rotational discontinuities (RDs), slow shocks (SSs), slow expansion waves (SEs), and a contact discontinuity (CD). These discontinuities and waves contribute to the plasma acceleration in the reconnection and lead to high-speed flows. The presence of rotational discontinuities have frequently been observed at the magnetopause, across which the tangential magnetic field undergoes a rotation similar to that predicted by the ideal MHD [*Lin and Lee*, 1993b]. In resistive MHD simulations for an asymmetric reconnection layer [*Lin et al.*, 1992; *Lin and Lee*, 1993a; *Lin and Lee*, 1993b; *Lin and Lee*, 1999; *Wu*, 1988; *Wu*, 1990], the RD is replaced by an intermediate shock (IS) in the antiparallel reconnection with the guide magnetic field $B_y = 0$, and by a time-dependent intermediate shock in the component reconnection with $B_y \neq 0$. The time-dependent intermediate shock, however, evolves with time toward the RD with the same field-rotation angle, although its width increases with time due to the finite resistivity [*Lin and Lee*, 1992; *Lin and Lee*, 1993b; *Wu and Kennel*, 1992].

[3] The structure of the discontinuities in the reconnection layer varies according to the magnetic field and plasma conditions on the two sides of the current sheet. Previous studies have shown that the structure of the reconnection layer is determined by the symmetry conditions across the current sheet, the plasma beta, and the magnitude of the guide field B_y [*La Belle-Hamer et al.*, 1994; *Lin and Lee*, 1993a; *Lin and Lee*, 1993b; *Lin and Lee*, 1994; *Sun et al.*, 2005]. Another important factor that can significantly change the reconnection layer is the flow shear across the layer. As the magnetosheath plasma blows into the magnetosphere, it induces a velocity shear whose magnitude and direction change with the position on the magnetopause. The shear flow can exist at the flanks or in the high latitudes of the magnetopause. It has been reported that accelerated flows and rotational discontinuities exist in reconnections at the flank and the dawn tail of the magnetopause, and the

[1]State Key Laboratory of Materials Modification by Beams, Department of Physics, Dalian University of Technology, Dalian, China.
[2]College of Advanced Science and Technology, Dalian University of Technology, Dalian, China.
[3]Physics Department, Auburn University, Auburn, Alabama, USA.

0148-0227/06/2006JA011812

observed reconnection layer structure is often more complicated than that on the dayside magnetopause where little flow is present in the magnetosheath [*Gosling et al.*, 1986; *Gosling et al.*, 1991]. Numerical simulations have been carried out to understand the effects of shear flows tangential to the antiparallel magnetic fields B_z [*La Belle-Hamer et al.*, 1994; *La Belle-Hamer et al.*, 1995; *Lin and Lee*, 1994; *Xie and Lin*, 2000]. La Belle-Hamer et al. [*La Belle-Hamer et al.*, 1995] found from their two-dimensional (2-D) resistive MHD simulations that in the presence of sheared plasma flow, an IS can form in a reconnection layer with equal magnetic field and density on the two sides of the initial current sheet, and in a reconnection layer with an asymmetric magnetic field and density the presence of IS can switch from one side to the other of the reconnection layer if the shear flow speed is greater than a critical value.

[4] The one-dimensional (1-D) hybrid simulation by *Lin and Lee* [1994] also demonstrated that a threshold velocity V^* exists, in such a way, when the magnetosheath flow speed is below (above) V^*, the rotational discontinuity with a larger field rotation angle is located on the magnetosheath (magnetospheric) side. The threshold value is nearly equal to the difference between the Alfvén speeds in the magnetosphere and the magnetosheath. Nevertheless, the sheared flow in all the previous researches is assumed to be in the direction tangential to the antiparallel component of the magnetic field.

[5] In fact, owing to the various orientations of the magnetic field on the magnetosheath and the magnetospheric sides of the magnetopause boundary layer, recent observations indicate that reconnections in the magnetosphere are often associated with a sheared plasma flow perpendicular to the antiparallel magnetic field component B_z [*Fedorov et al.*, 2003; *Fusilier et al.*, 2000; *Phan et al.*, 2001]. Rotational discontinuities were also observed in such reconnections. The effects of a perpendicular shear flow on the structure of the reconnection layer was discussed recently by *Sun et al.* [2005] using a resistive MHD simulation. It was shown that because of the sheared flow ΔV_y across the current layer, time-dependent intermediate shocks are present in the reconnection layer even in an antiparallel reconnection ($B_y = 0$). For a component reconnection, the structure of the reconnection layer also changes significantly with the shear flow in V_y: such shear flow can lead to the reversal of the rotation sense of the tangential magnetic field through the reconnection layer. The critical value of the shear flow for the occurrence of this field reversal was discussed [*Sun et al.*, 2005]. This study, however, did not address the detailed structure of the reconnection layer as a function of the shear flow in positive or negative V_y, nor did it include the simultaneous presence of shear flow components both parallel with and perpendicular to B_z.

[6] In this paper, we conduct a systematic resistive MHD simulation for the structure of reconnection layers at the magnetopause in the presence of shear flows in V_y and V_z. The critical shear flows and the corresponding reconnection-layer structures are discussed for the general reconnection cases, in which the guide field $B_y \neq 0$. The simulation model is described in section 2. Section 3 presents the simulation results for cases with shear flows in V_y perpendicular to the antiparallel magnetic field. Cases with shear flows in both V_y and V_z will be presented in section 4. Finally, a summary is given in Section 5.

2. Simulation Model

[7] A 1-D resistive MHD simulation code is used to simulate the evolution of an initial current sheet in the presence of a magnetic field component B_n normal to the current sheet, which is a Riemann problem corresponding to magnetic reconnection [*Jeffrey and Taniuti*, 1964]. The following set of MHD equations are solved in the simulation.

$$\frac{\partial \rho}{\partial t} + \nabla \cdot (\rho \mathbf{V}) = 0 \tag{1}$$

$$\frac{\partial (\rho \mathbf{V})}{\partial t} + \nabla \cdot \left[\left(P + \frac{\mathbf{B}^2}{2\mu_0} \right) + \rho \mathbf{V}\mathbf{V} - \frac{\mathbf{B}\mathbf{B}}{\mu_0} \right] = 0 \tag{2}$$

$$\frac{\partial \varepsilon_T}{\partial t} + \nabla \cdot \left[\left(\frac{\rho \mathbf{V}^2}{2} + \frac{P}{\gamma - 1} + P \right) \mathbf{V} + \frac{1}{\mu_0} \mathbf{E} \times \mathbf{B} \right] = 0 , \tag{3}$$

$$\frac{\partial \mathbf{B}}{\partial t} = -\nabla \times \mathbf{E} \tag{4}$$

$$\nabla \cdot \mathbf{B} = 0, \tag{5}$$

with

$$\varepsilon_T = \frac{1}{2} \rho \mathbf{V}^2 + \frac{P}{\gamma - 1} + \frac{\mathbf{B}^2}{2\mu_0} \tag{6}$$

and

$$\mathbf{E} = -\mathbf{V} \times \mathbf{B} + \eta \mathbf{J}, \tag{7}$$

where ρ, $\mathbf{V}$, $\mathbf{B}$, $\mathbf{J}$, and P are the plasma density, flow velocity, magnetic field, current density, and thermal pressure, respectively, and η is the resistivity.

[8] The solution of the Riemann problem corresponds to a quasi-steady reconnection configuration in which the separatrix angle is small. In this paper the normal of the initial current sheet is assumed to be in the x-direction, the antiparallel component of the magnetic field is in the z-direction, and the common magnetic guide field is in the y-direction. Assume that the initial current sheet is located at $x = 0$. Let the subscripts 1 and 2 stand for the quantities on the magnetosheath ($x < 0$) and magnetospheric ($x > 0$) sides of the current sheet, respectively. Finite flow shears ΔV_y and ΔV_z are applied across the current sheet. The simulation is carried out in the frame of reference in order that the flows on the two sides of the initial current sheet $\mathbf{V_1} = -\mathbf{V_2} = \mathbf{V_0}$. The Riemann problem is solved for a 1-D ($\partial/\partial y = \partial/\partial z = 0$) system. Without the normal magnetic field, the initial current sheet is a tangential discontinuity, through which the total (magnetic plus thermal) pressure is balanced as

$$P + \frac{\mathbf{B}^2}{2\mu_0} = const. \tag{8}$$

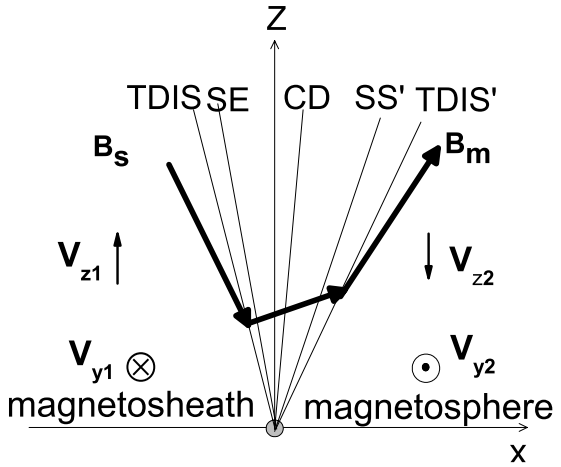

Figure 1. The sketch of simulation coordinate system for a case with $V_{y0} > 0$ and $V_{z0} > 0$. The fronts TDIS and TDIS′ indicate the time-dependent intermediate shocks on the magnetosheath and magnetospheric sides of the reconnection layer, respectively.

In the presence of the finite $B_n = B_x$, which is a constant in the 1-D system according to $\nabla \cdot \mathbf{B} = 0$, the current sheet disintegrates instantly at time $t > 0$, resulting in the formation of MHD discontinuities and waves, which propagate away from the current sheet.

[9] Figure 1 shows a sketch of the corresponding structure of the reconnection layer in the 2-D plane for $V_{y1} = -V_{y2} = V_{y0} > 0$ and $V_{z1} = -V_{z2} = V_{z0} > 0$. The dimension z corresponds to the time t in the 1-D Riemann problem. The profiles of the initial velocity are described by

$$V_y(x) = -V_{y0} \tanh\left(\frac{x}{a}\right), \tag{9}$$

and

$$V_z(x) = -V_{z0} \tanh\left(\frac{x}{a}\right). \tag{10}$$

Here, a is half width of the initial current sheet and equal to 5 grid points.

[10] The normal field component is chosen as $B_x = 0.25$. The initial z-component of the magnetic field is given by

$$B_{z0}(x) = \frac{1}{2}(B_{z2} + B_{z1}) + \frac{1}{2}(B_{z2} - B_{z1}) \tanh\left(\frac{x}{a}\right), \tag{11}$$

where B_{z1} and B_{z2} are the B_z components of the asymptotic fields. The initial tangential magnetic field strength $B_{t0}(x)$ also follows the hyperbolic tangent profile that connects B_{t1} and B_{t2}, the tangential magnetic fields on the two sides of the current sheet. The common guide field $B_{y1} = B_{y2} \equiv B_{y0}$. The presentation in this paper is mainly focused on the shear flow effects at fixed $B_{y0} = 0.5$, although the results with $B_{y0} < 0$ are discussed briefly for comparison. The profile of initial B_y as a function of x is given by

$$B_y(x) = \left[B_{t0}^2(x) - B_z^2(x)\right]^{1/2}. \tag{12}$$

[11] In the following, the density is normalized by the density ρ_2 in the magnetosphere, magnetic field by the tangential magnetic field B_{z2}, the plasma velocity by the tangential Alfvén velocity $V_{Az2} = B_{z2}/\sqrt{\mu_0 \rho}$, and the pressure by $\frac{B_{z2}^2}{\mu_0}$. The length is normalized by the half-width a of the current sheet, the time by $t_{A2} = \frac{a}{V_{Az2}}$, and the resistivity η by $\mu_0\, a V_{Az2}$. The current density is expressed in units of $\frac{B_{z2}}{\mu_0 a}$. The resistivity is set as $\eta = 0.04$. The number of grid points in the simulation domain is 2000 to 8000. A free boundary condition $\frac{\partial}{\partial x} = 0$ is used at $x = \pm L_x/2$, where L_x is the length of the simulation domain.

3. Simulation Results for Cases With Shear Flow Speeds $V_{y0} \neq 0$ and $V_{z0} = 0$

[12] In this section we take into account only the effects of shear flows in V_y on the structure of the reconnection layer. First, let $V_{y0} > 0$. Figure 2 shows the simulation results of case 1 with the shear flow speed $V_{y0} = 0.1$ at $t = 2120$. In case 1, $\rho_1 = 10\rho_2$, $B_{z1} = -B_{z2}$, $B_{y0} = 0.5$, and $\beta_2 = 0.2$, as in an asymmetric current sheet at the magnetopause. At this time, two weak fast expansion waves (FE and FE′) have already propagated out of the reconnection layer. In the main reconnection layer, on the left side appear a strong time-dependent intermediate shock TDIS (from a to b) and a slow shock SS (from b to c), and on the right side a weak time-dependent intermediate shock TDIS′ (from i to h) and a slow shock SS′ (from f to g). A contact discontinuity CD (around e) stands in the middle of the reconnection layer. Across the time-dependent intermediate shocks, the tangential magnetic field changes the direction. The hodogram of the tangential magnetic field for case 1 is shown in the top left plot of Figure 3. In the tangential plane, the field (B_y, B_z) rotates from both sides through TDIS and TDIS′ to a common angle, which corresponds to the magnetic fields at the two slow shocks. TDIS on the magnetosheath side possesses a field rotation angle of $\sim$120°, which is much larger than a field rotation angle of $\sim$7° of TDIS′ on the magnetospheric side. Although the time-dependent intermediate shocks are not steady in the resistive MHD, with their widths increasing with time and the slightly nonconstant density and magnetic field strength, the Walén relation for rotational discontinuities is roughly satisfied across these structures.

[13] Conversely, the magnetic field direction does not change across the slow shocks, but the field magnitude decreases while the density is enhanced. The tangential field decreases to a minimum across SS and SS′, while the shock coplanarity condition is satisfied. The Rankine-Hugoniot (RH) jump conditions [*Landau and Lifshitz*, 1960] are satisfied at both slow shocks. The plasma is greatly accelerated, in V_z, by magnetic forces in the discontinuities from both sides of the reconnection layer. Across the CD, only the density and temperature change.

[14] Now let us note that the velocity change $\Delta V_y < 0$ across TDIS′ from upstream to downstream, while $\Delta B_y > 0$ corresponding to the field rotation in Figure 3, as expected from the Walén relation $\Delta V_y \simeq -\Delta V_{Ay}$ for the wave vector $\mathbf{k} \| \mathbf{B_x}$ at TDIS′ propagating to the right, where V_{Ay} is the y-component of the Alfvén velocity. The component V_y then changes toward the positive direction across SS′ behind

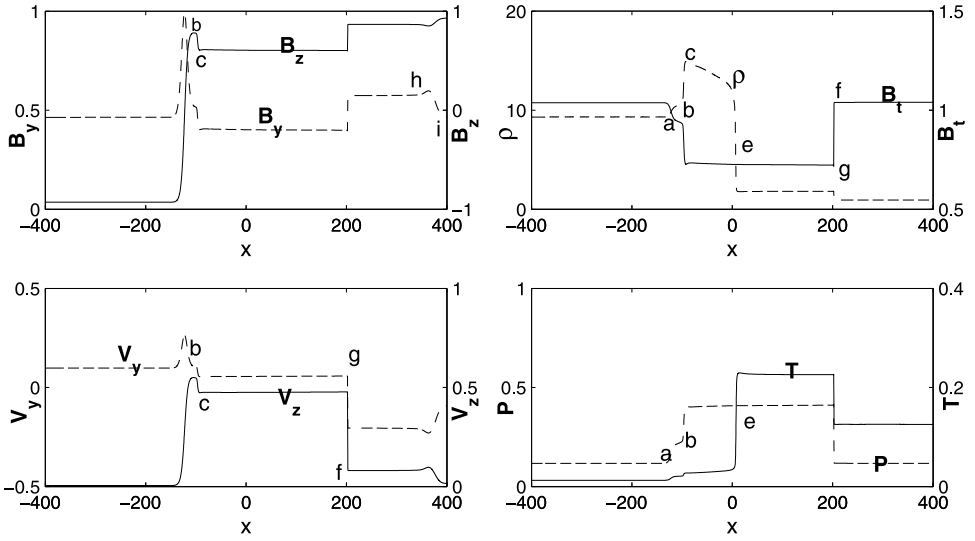

Figure 2. Spatial profiles of various quantities in case 1 with shear flow speed V_{y0} = 0.1: density ρ, tangential magnetic field force B_t, velocity V_y and V_z, pressure P and temperature T, and magnetic field B_y and B_z, at t = 2120.

TDIS′, where $\Delta B_y < 0$, to reach a common value at the center of the reconnection layer. If the initial shear flow speed V_{y0} increases, and thus V_{y2} at the right (magnetospheric) boundary is more negative, ΔB_y and thus the rotation angle of the tangential magnetic field across TDIS′ have to decrease, so that the negative ΔV_y is not too strong to satisfy the matching of V_y at the center. Therefore as V_{y0} increases, the field rotation angle across TDIS′ becomes smaller.

[15] Indeed, the structure of the reconnection layer is found to vary significantly with the initial shear flow speed,

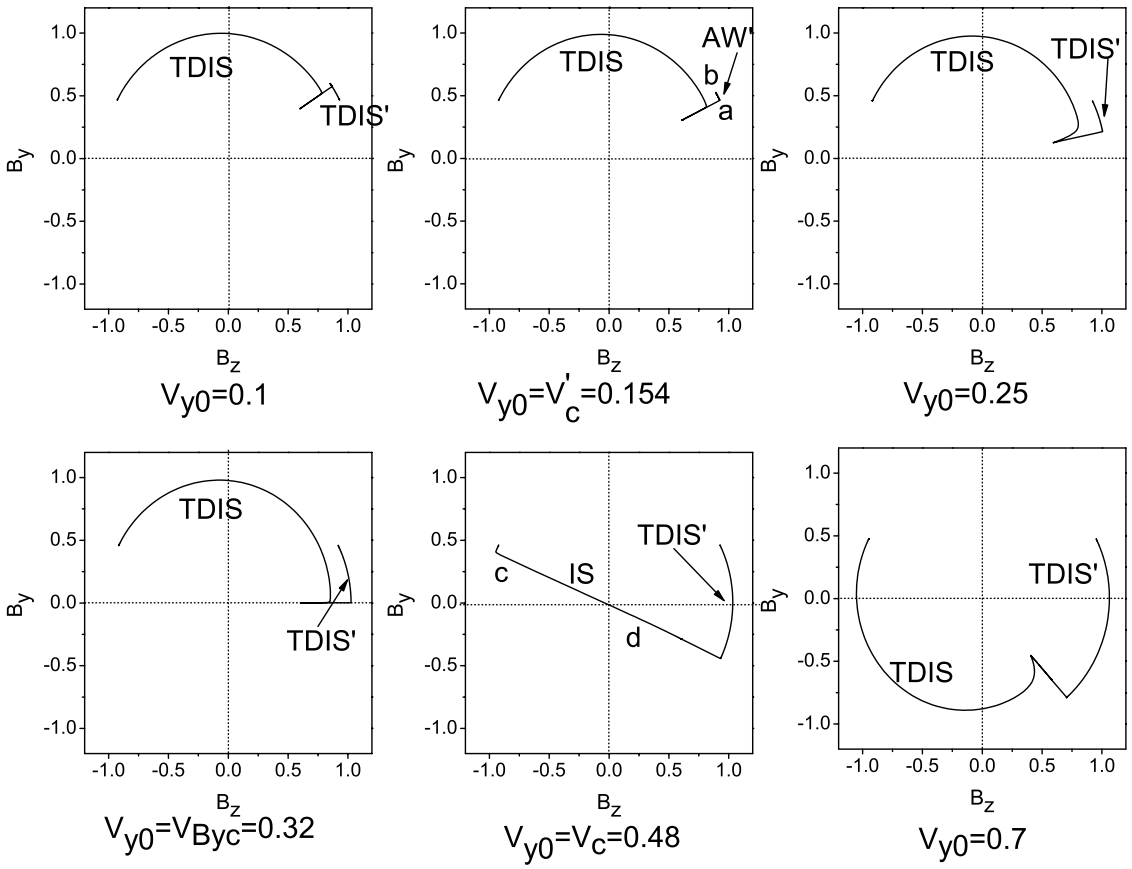

Figure 3. Hodograms of the tangential magnetic field (B_y-B_z) for cases with various shear flow speed V_{y0} = 0.1 to 0.7.

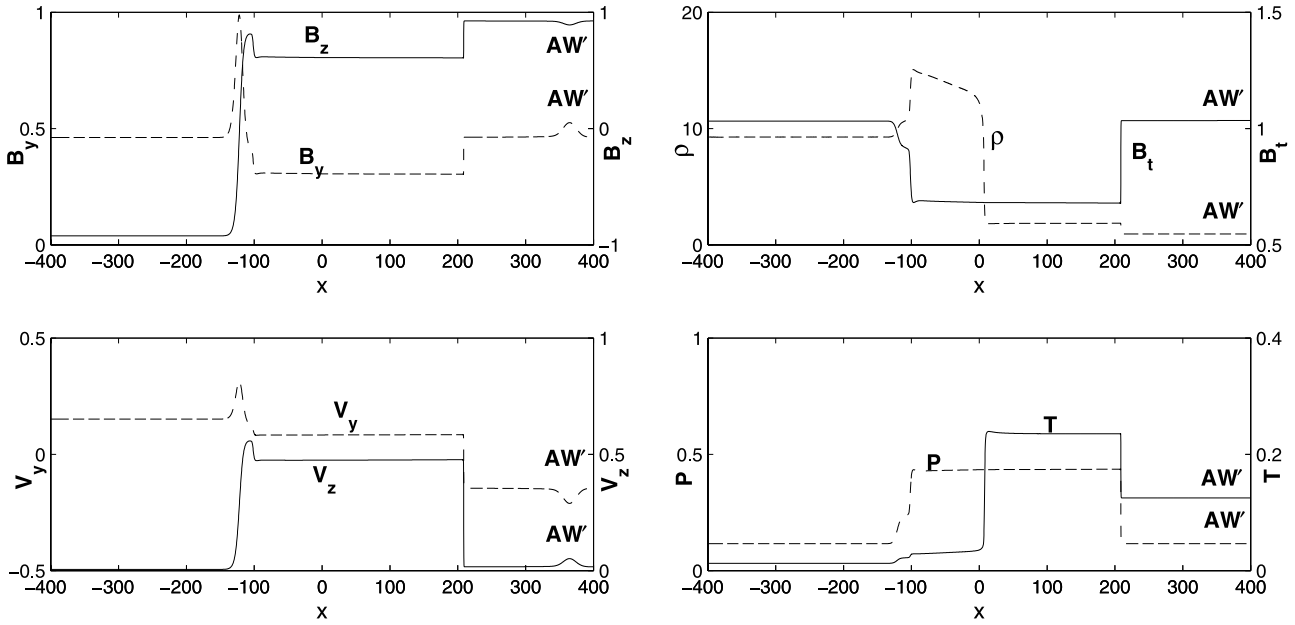

Figure 4. Spatial profiles of ρ, B_t, V_y, V_z, B_y, B_z, P, and T in case 2 with $V_{y0} = V'_c = 0.154$, the critical case when the weak TDIS′ is replaced by an Alfvén wave pulse.

as shown in the field hodograms in Figure 3 for various V_{y0}. The field rotation angle across TDIS′ decreases with V_{y0}, while the field rotation angle across the strong TDIS increases with V_{y0}. At a critical value $V_{y0} = V'_c = 0.154$, TDIS′ is replaced by a new Alfvén wave pulse AW′, across which the tangential magnetic field does not change direction (from a to b and then back to a), as seen in the top middle plot of Figure 3. Moreover, as $V_{y0} > V'_c$, the field rotation sense across TDIS′ is found to reverse, toward the direction of decreasing B_y. As the shear flow speed keeps increasing to $V_{y0} = V_{Byc} = 0.32$, the downstream field of TDIS′ (and TDIS) reaches $B_y = 0$. In this situation, B_y remains zero in SS and SS′ from upstream to downstream. Meanwhile, as the field rotation reverses across TDIS′ when $V_{y0} > V'_c$, the rotation angle across the strong TDIS still increases with V_{y0} in order to match the field at the center of the reconnection layer. At a critical value $V_{y0} = V_c = 0.48$, the strong TDIS is replaced by a new discontinuity with a 180° change in the direction of the tangential magnetic field. This new discontinuity is an intermediate shock (IS), in which the tangential magnetic field passes through the origin, and the field is thus coplanar, as seen in Figure 3. Finally, if $V_{y0} = 0.7 > V_c$, the strong TDIS also reverses its field rotation sense so that the rotation angle of the tangential field across TDIS is smaller than 180°, consistent with previous MHD results of minimum-angle rotation of magnetic field in a current sheet or rotational discontinuity [e.g., *Miura*, 2002]. As a result, B_y changes toward negative values from both sides of the reconnection layer, as shown in the bottom right hodogram of Figure 3. Note that the slow shocks in this hodogram are still evolving toward a coplanar structure. In later times, the tangential field will follow a fuller arc through each time-dependent intermediate shock so that the field changes across the coplanar slow shocks will be along a straight line in the hodogram.

[16] In order to illustrate the presence of the new structures AW′ and IS in the above-mentioned critical cases, we show the spatial profiles of various quantities in these cases in the next several figures. Figure 4 shows the spatial profiles of ρ, B_t, V_y, V_z, B_y, B_z, P, and T for case 2 with $V_{y0} = V'_c = 0.154$. The first structure on the right side corresponds to the Alfvén wave AW′, with wave pulses in the transverse components of the magnetic field and flow velocity. The density, pressure, and magnetic field strength are conserved through this pulse. Note that the Alfvén Mach number of AW′ is about unity.

[17] The time evolutions of spatial profiles of tangential magnetic field B_z and density ρ for case 3 with $V_{y0} = 0.3 < V_c$, case 4 with $V_{y0} = V_c = 0.48$, and case 5 with $V_{y0} = 0.8 > V_c$ are presented in Figure 5, Figure 6, and Figure 7, respectively. In case 3 with the shear flow speed $V_{y0} = 0.3$, a time-dependent intermediate shock TDIS and a slow expansion wave SE emerge on the left side in early times, but a slow shock SS is present behind TDIS at $t > 2094$ as the TDIS evolves with time. This group of nonsteady TDIS, SS, and SE continues to evolve while TDIS keeps widening and SE gradually disappears, as found in the MHD simulations for the magnetopause reconnection layer without shear flow in V_y [*Lin and Lee*, 1993b]. As $t \rightarrow \infty$, the TDIS evolves to a rotation discontinuity with an infinite width.

[18] Nevertheless, when the shear flow speed V_{y0} reaches the critical value V_c, as shown in Figure 6 for case 4, the group of time-dependent structures on the left side of the reconnection layer is replaced by a steady intermediate shock, IS, followed by a slow expansion wave. The width of the IS does not change with time. At $t = 3372$, the upstream tangential magnetic field, density, pressure, and the normal inflow velocity in the shock frame are found to be $B_{tu} = 1.03$, $\rho_u = 9.26$, $P_u = 0.115$, and $v_{nu} = 0.086$, respectively, and the downstream values are $B_{td} = 0.403$, $\rho_d = 15.43$, $P_d = 0.595$, and $v_{nd} = 0.053$. The direction of the tangential magnetic field changes by 180°, as also seen from c to d in the lower middle hodogram in Figure 3. The RH jump relations are found to be satisfied for this intermediate

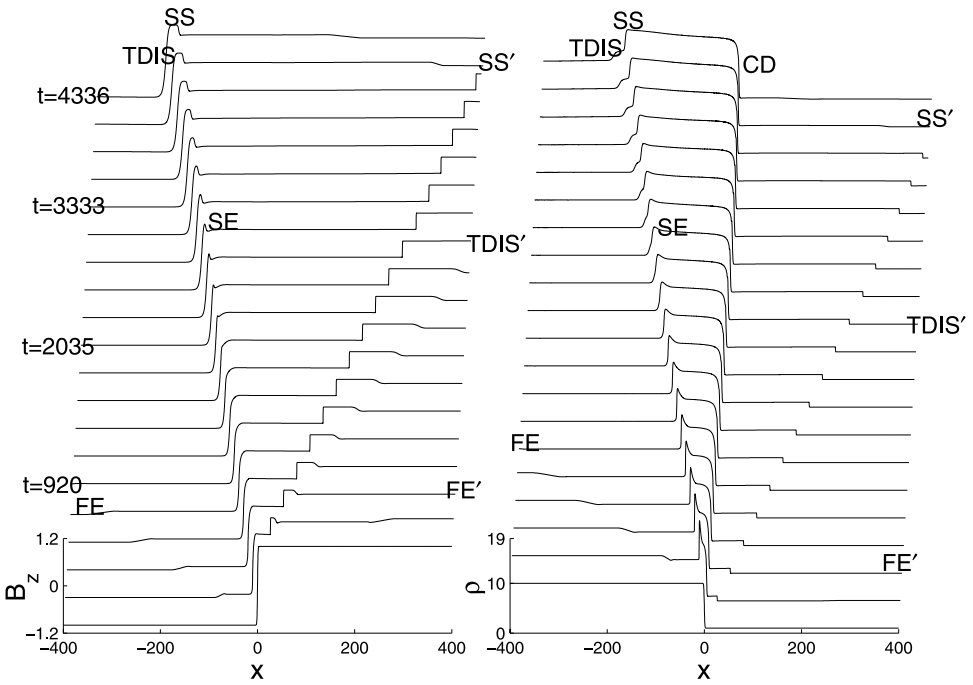

Figure 5. Evolution of B_z and ρ profiles in a time sequence for case 3 with $V_{y0} = 0.3$.

shock, with Mach number $M_I = 1.048$. Finally, in case 5 with $V_{y0} > V_c$, not only the field rotation sense is reversed on the left side of the reconnection layer, as discussed earlier, but the main structures on the left side are again a TDIS followed by slow mode discontinuities, as seen in Figure 7.

[19] The solid triangles and diamonds in Figure 8 show the critical speeds V'_c, V_{Byc}, and V_c obtained in the simulation as a function of the magnetosheath to magnetospheric density ratio ρ_1/ρ_2, until $\rho_1/\rho_2 = 100$ as in a highly asymmetric magnetopause boundary layer. The symmetric case with $\rho_1/\rho_2 = 1$ is also plotted. Since the jumps of physical quantities in the reconnection layer obtained from the resistive MHD simulation should approach the ideal MHD results as $t \rightarrow \infty$, we have also performed an analytical search for the critical speeds based on the ideal MHD equations [*Lin and Lee*, 1993b]. The three solid lines in Figure 8 represent the critical speeds based on the ideal MHD approximation. We note that the rotation angles of

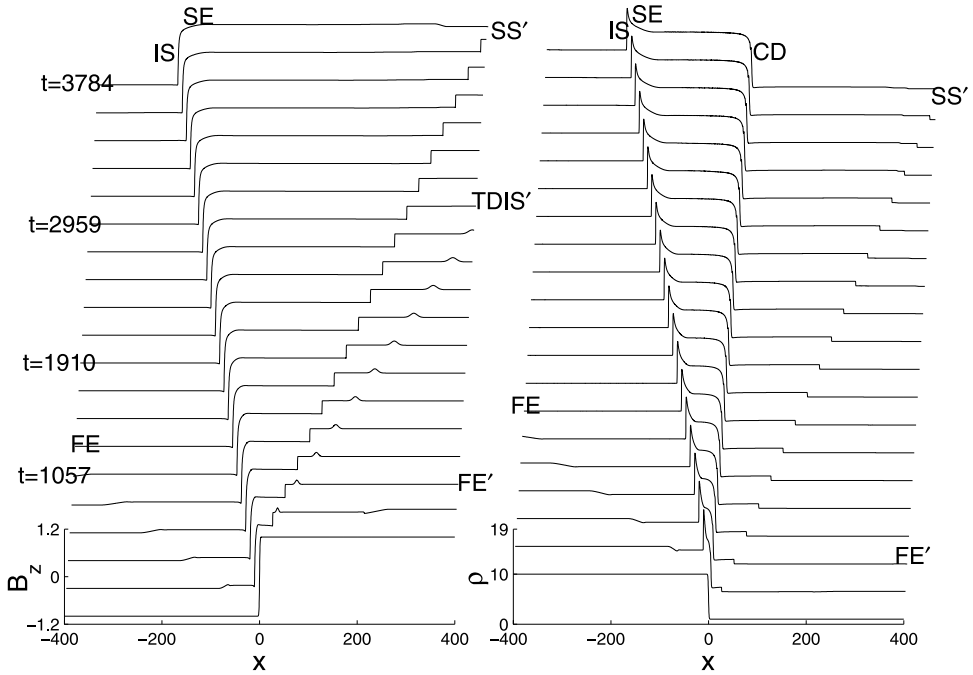

Figure 6. Evolution of B_z and ρ profiles in a time sequence for case 4 with $V_{y0} = V_c = 0.48$.

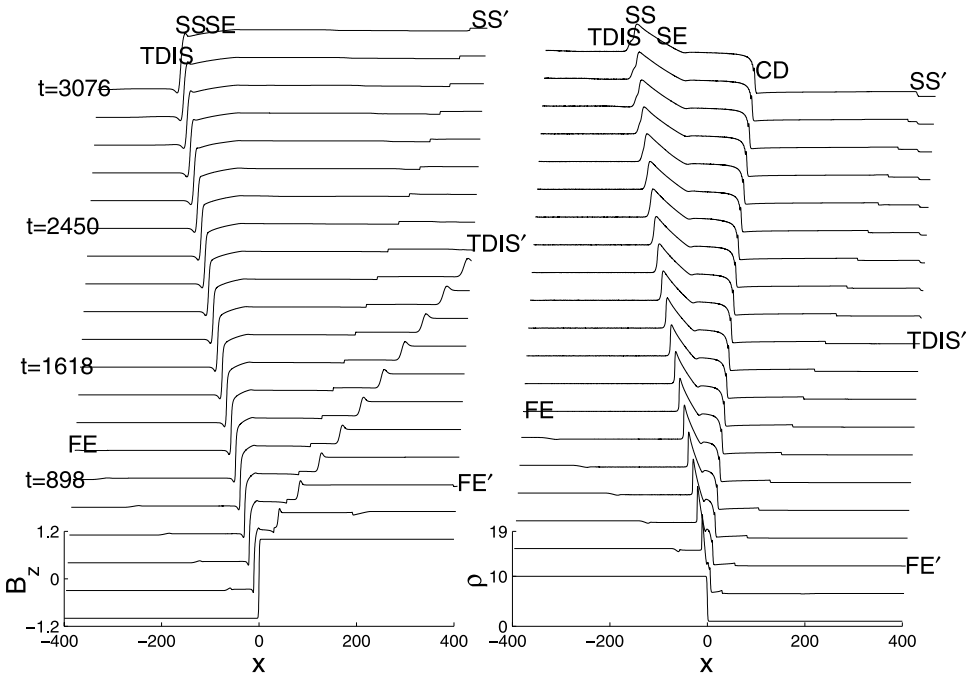

Figure 7. Evolution of B_z and ρ profiles in a time sequence for case 5 with $V_{y0} = 0.8$.

tangential magnetic field obtained from the resistive MHD are in good agreement with the ideal MHD theory. As V_{y0} increases, the weak TDIS′ on the magnetospheric side reverses the field rotation sense first at $V_{y0} > V'_c$, while an AW′ replaces TDIS′ in the critical case with $V_{y0} = V'_c$ as shown above. Then at $V_{y0} = V_{Byc}$, the downstream field of TDIS′ (and TDIS) reaches $B_y = 0$, and so does the tangential field throughout SS and SS′. Finally, as V_{y0} further increases to $V_{y0} > V_c$, the strong TDIS on the magnetosheath side also reverses the field rotation sense, whereas in the critical case with $V_{y0} = V_c$ an IS replaces TDIS. It is revealed from Figure 8 that the critical speed V_c hardly changes with the density ratio in a vast range of ρ_1/ρ_2, remaining at $V_c \approx 0.5$. Both the critical speeds V_{Byc} and V'_c, however, decrease with ρ_1/ρ_2 drastically for $\rho_1/\rho_2 < 20$.

[20] Note that when ρ_1/ρ_2 approaches 1, the three critical speeds $V_c = V_{Byc} = V'_c$. The symmetric case with $\rho_1/\rho_2 = 1$, however, is a singular case in which the magnetic field is always symmetric, about $x = 0$, and thus the tangential magnetic field does not reach $B_y = 0$ downstream of the time-dependent intermediate shocks. As discussed by *Sun et al.* [2005] based on an analytical derivation from the shock jump conditions, in the symmetric case the critical speeds are around $V_c = V'_c = V_{Ay1} = V_{Ay2} = 0.5$.

[21] On the other hand, we have also simulated the cases with $V_{y0} < 0$, so that $V_{y1} < 0$ in the magnetosheath. Figure 9 shows the profiles of ρ, B_t, V_y, V_z, P, and T in case 6 with $V_{y0} = -0.1$ at $t = 2180$. Similar to case 1 with $V_{y0} = 0.1$ shown in Figure 2, six discontinuities are present in the resulting reconnection layer, including TDIS, SS, SE, CD, SS′, and TDIS′. In contrast to case 1, however, the velocity jump now from i to h (still with $\Delta V_y < 0$) is not in the direction that enhances the flow difference from V_y at the center of the reconnection layer. Thus if $|V_{y0}|$ is increased, the MHD matching conditions can still be satisfied without changing the field rotation senses. Figure 10 shows the magnetic field hodograms for cases with $V_{y0} = -0.1$, -0.3, and -0.7. We see that as $|V_{y0}|$ increases, the strength $\Delta\mathbf{B}$ of TDIS′ is also enhanced in order to decrease V_y and increase V_z across the discontinuities from the right side. Correspondingly, the strength of TDIS decreases. No field reversal is found for $V_{y0} < 0$. Moreover, a large $|V_{y0}|$ is found to result in the presence of fast shocks and slow expansion waves on both sides of the reconnection layer in its asymptotic solution, due to the monotonic change of V_y from left to right in order to match the large shear flow ΔV_y. Note that at $V_{y0} \simeq 1.1$, no

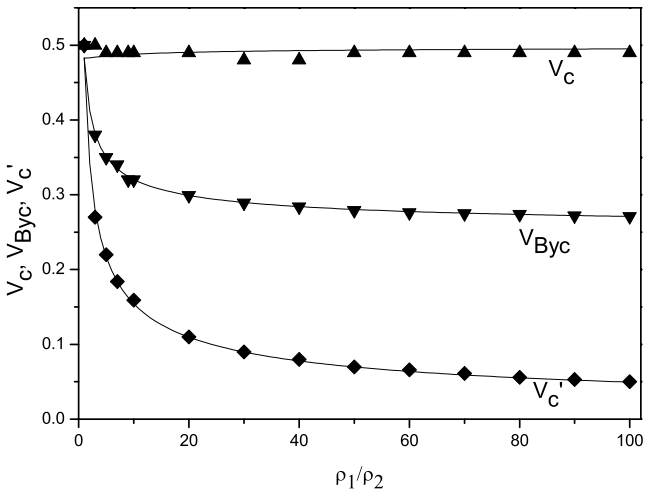

Figure 8. Solid triangles and diamonds indicate the variation of the critical speeds V_c, V_{Byc}, and V'_c with the magnetosheath-to-magnetospheric density ratio ρ_1/ρ_2 obtained from the resistive MHD simulation. Solid lines indicate the corresponding critical speeds obtained from the ideal MHD approximation.

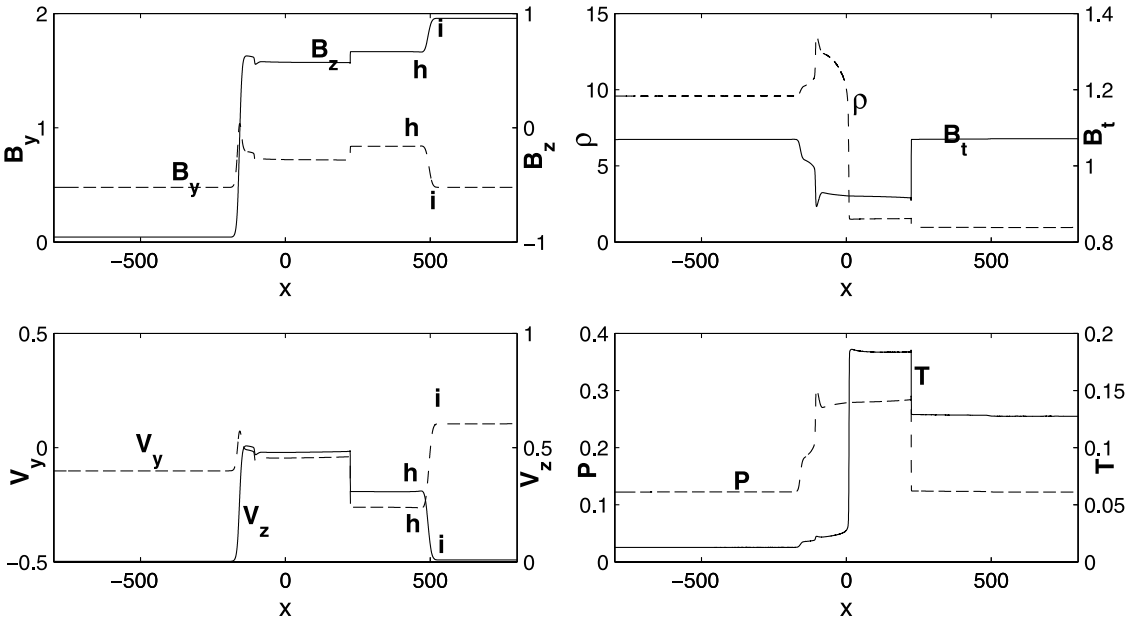

Figure 9. The profiles of ρ, B_t, V_y, V_z, P, T with shear flow $V_{y0} = -0.1$.

solution is found for the Riemann problem, as ρ of downstream of the strong slow expansion waves drops to zero.

4. Simulation Results for Cases With $V_{y0} \neq 0$ and $V_{z0} \neq 0$

[22] In this section, we consider the effects of finite shear flow velocities in both V_y and V_z. In particular, the magnetic field rotation in the reconnection layer is investigated. Let us first consider the cases with $V_{y0} > 0$ and $V_{z0} > 0$, where $V_{z0} > 0$ corresponds to a magnetosheath flow V_{z1} parallel to the magnetic tension force. In the following, the shear flow speed V_{z0} is fixed at $V_{z0} = 0.1$ or $V_{z0} = 0.5$, while V_{y0} is varied.

[23] While the shear flow in V_y does not change the symmetry condition of the reconnection layer [*Sun et al.*,

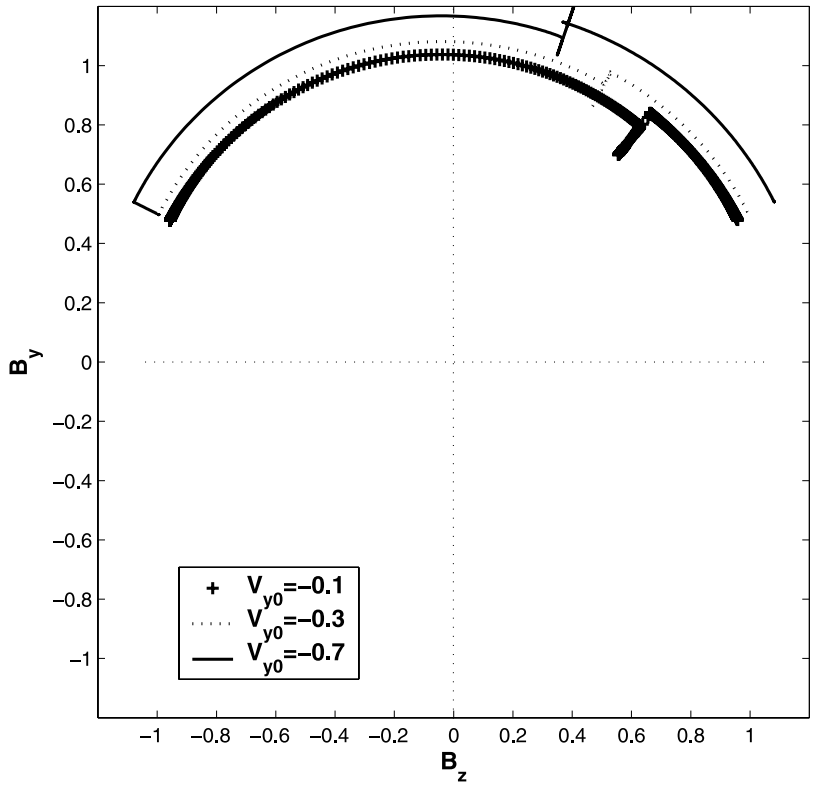

Figure 10. Hodograms of tangential magnetic field B_z-B_y for cases with $V_{y0} = -0.1$, -0.3 and -0.7.

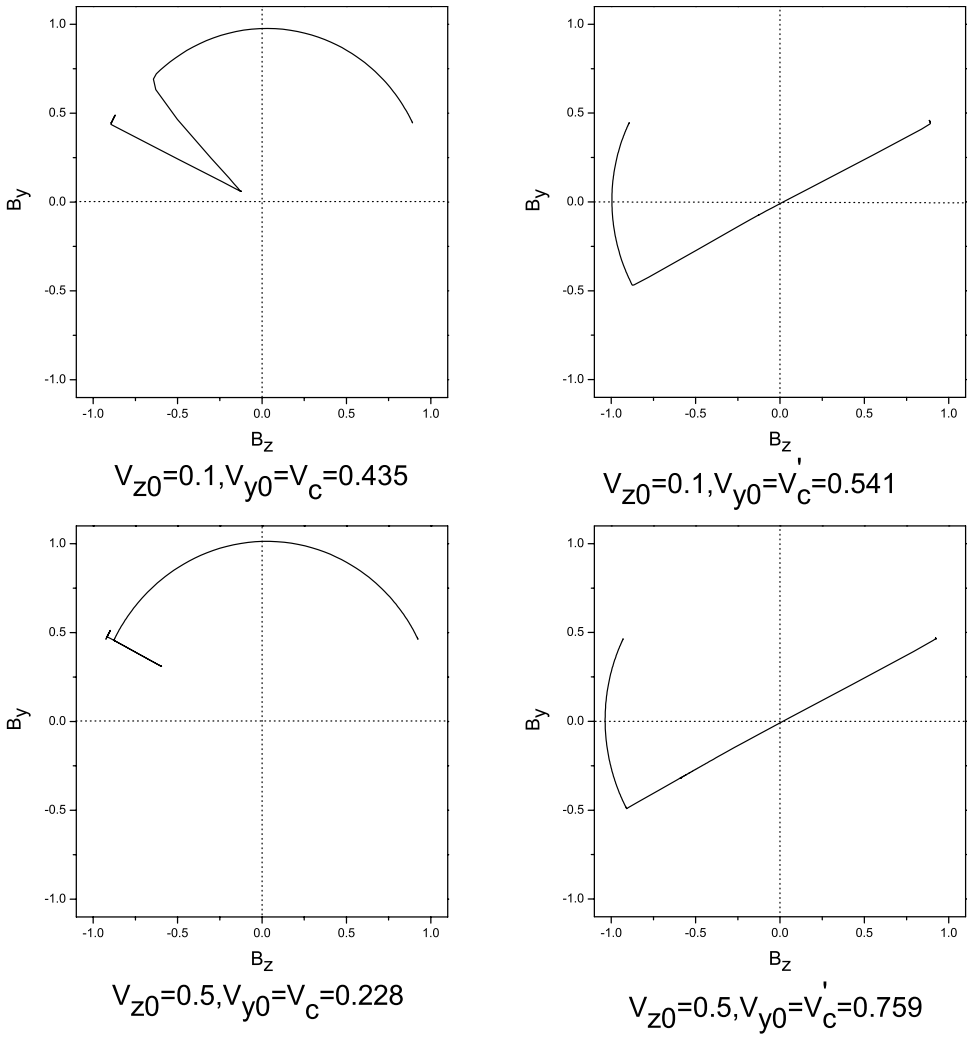

Figure 11. Magnetic field hodogram for cases with symmetric magnetic field and equal density on the two sides of the reconnection layer at various critical V_{y0}, under $V_{z0} = 0.1$ and 0.5.

2005], the presence of the shear flow in V_z does. For example, for an initial current sheet with symmetric magnetic fields and equal plasma densities on the two sides, a finite V_{z0} breaks the symmetry of the reconnection layer about $x = 0$(and $z = 0$) [*La Belle-Hamer et al.*, 1994; *La Belle-Hamer et al.*, 1995]. Therefore, the presence of a finite V_{z0} alters the magnetic structure of the reconnection layer and thus various critical speeds in V_{y0}. Figure 11 shows the magnetic field hodograms corresponding to the critical cases with $V_{y0} = V_c$ and $V_{y0} = V'_c$, under $V_{z0} = 0.1$ and 0.5, for the case with symmetric $\rho_1 = \rho_2$ and $B_{z1} = -B_{z2}$ at the initial current sheet, and $\beta_1 = \beta_2 = 0.2$. In such cases, since $V_{z1} = V_{z0} > 0$ on the left side is parallel to the magnetic tension force or the accelerated plasma velocity, and $V_{z2} = -V_{z0} < 0$ on the right side is antiparallel to the tension force, a discontinuity with a smaller (larger) field line kink is required on the left (right) side to accelerate the plasma to the common $V_z > 0$ near the center. Therefore TDIS′ on the right side is stronger than TDIS on the left side [*La Belle-Hamer et al.*, 1995; *Lin and Lee*, 1994]. The results for $V_{z0} = 0.1$ are presented in the top row of Figure 11. The top left plot of Figure 11 indicates the critical speed $V_c = 0.435$, so that when $V_{y0} > 0.435$ the field rotation sense in the weak TDIS (on the left) reverses. As V_{y0} further increases, the case shown in the top right plot of Figure 11 with $V_{y0} = V'_c = 0.541$ corresponds to the critical case in which the strong TDIS′ (on the right) is replaced by a coplanar IS. If $V_{y0} > 0.541$, the discontinuity TDIS′ reappears on the right but with a reversed field rotation sense.

[24] For a larger $V_{z0} = 0.5$, the weak (strong) TDIS on the left (right) becomes even weaker (stronger) than in the cases with $V_{z0} = 0.1$, so that the critical speed V_c is smaller, equal to 0.228, and the critical speed V'_c is larger, equal to 0.759.

[25] If the initial current sheet is asymmetric, e.g., with $\rho_1 > \rho_2$ as at the magnetopause, the effects of the asymmetric density and the finite shear flow in V_z will compete with each other for the formation of the strong or weak time-dependent intermediate shocks [*La Belle-Hamer et al.*, 1995]. Figure 12 shows the resulting field hodograms at various critical speeds of V_{y0} for the asymmetric case with $\rho_1 = 10\rho_2$ and $B_{z1} = -B_{z2}$, under $V_{z0} = 0.1$ and 0.5. As easily seen from Figure 12, the results for $V_{z0} = 0.1$ are very different from those for $V_{z0} = 0.5$. At lower speed $V_{z0} = 0.1$, the strong TDIS is present on the left side, similar to case 1 shown in Figure 2, due to the dominant effects of the asymmetric density. The critical speeds $V'_c = 0.2$ and $V_c =$

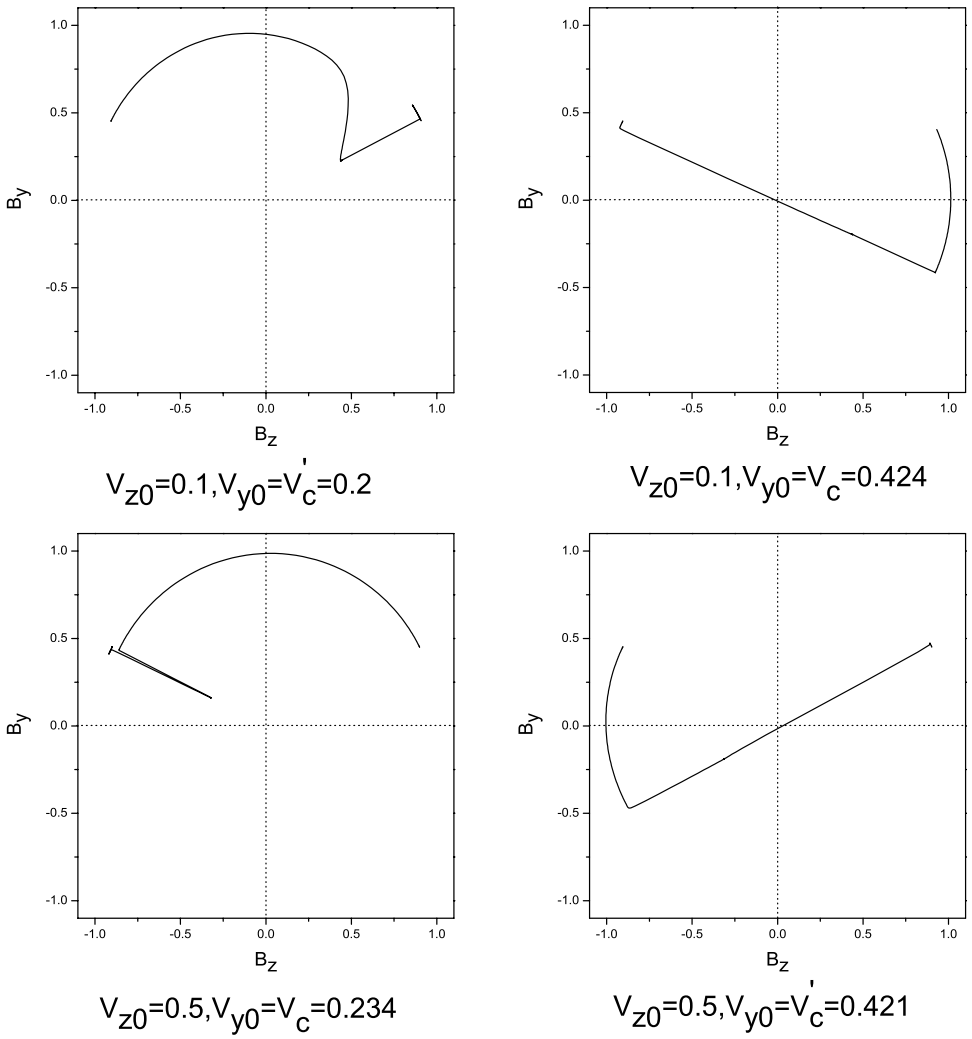

Figure 12. Same as Figure 11, but for asymmetric cases with $\rho_1 = 10\rho_2$.

0.424. At the higher $V_{z0} = 0.5$, however, the strengths of TDIS and TDIS′ have switched because of the dominant effect of the shear flow V_{z0} [*La Belle-Hamer et al.*, 1995; *Lin and Lee*, 1994]. The critical speeds are found to be $V_c = 0.234$ for the field reversal of the weak TDIS and $V'_c = 0.421$ for the field reversal of the strong TDIS′.

[26] If the direction of shear flow in V_y or V_z changes so that $V_{y0} < 0$ or $V_{z0} < 0$, the structure of the reconnection layer undergoes certain changes as discussed below in Figures 13, Figure 14, and Figure 15. Results of some cases with $V_{y0} < 0$ but $V_{z0} > 0$ are shown in the magnetic field hodograms in Figure 13. Similar to cases with $V_{z0} = 0$ shown in section 3, the time-dependent intermediate shocks in the reconnection layer do not reverse their field rotation senses as $|V_{y0}|$ increases when $V_{y0} < 0$. Likewise, even for $V_{z0} < 0$, the field rotation senses also do not change if $V_{y0} < 0$, as seen in Figure 15.

[27] The sign of V_{z0} also leads to significant changes in the structure of the reconnection layer. If $V_{z0} < 0$, the shear flow velocity V_{z1} in the magnetosheath, on the left side, is antiparallel with the magnetic tension force. So TDIS on the left side is always stronger than TDIS′ on the right, as both the asymmetric density and the shear flow facilitate the formation of the large-amplitude TDIS. Increasing $|V_{z0}|$ will not cause the interchange between the strengths of the two time-dependent intermediate shocks, as shown in Figure 14.

[28] The reversal of the field rotation sense in either TDIS or TDIS′, however, also occurs when $V_{z0} < 0$, provided $V_{y0} > 0$, as shown in Figure 14. Overall, the quantitative dependence of the critical speeds V_c and V'_c on both positive and negative V_{z0} is shown in Figure 16. Results for the case with symmetric magnetic field and density, $B_1 = B_2$ and $\rho_1 = \rho_2$, on the two sides of the initial current sheet are plotted in Figure 16a, whereas Figure 16b is for the case with asymmetric densities $\rho_1 = 10\rho_2$ and $B_1 = B_2$. The critical speeds $V_{y0} = V_c$ are depicted by the solid squares, while the critical speeds $V_{y0} = V'_c$ are plotted as open circles. We see that for the symmetric case, V'_c increases with V_{z0}, while V_c decreases with V_{z0}. The point $V_{z0} = 0$ separates cases with stronger or weaker TDIS on the left, so that a strong time-dependent intermediate shock emerges on the left side for $V_{z0} < 0$, but emerges on the right side for $V_{z0} > 0$. At $V_{z0} = 0$, the strengths of TDIS and TDIS′ are equal. For either sense of V_{z0}, the strong time-dependent intermediate shock becomes stronger and stronger as $|V_{z0}|$ increases, and meanwhile the weak time-dependent intermediate shock becomes weaker and weaker. Correspondingly, the critical speed $V_{y0} = V_c$ required for the field reversal in TDIS

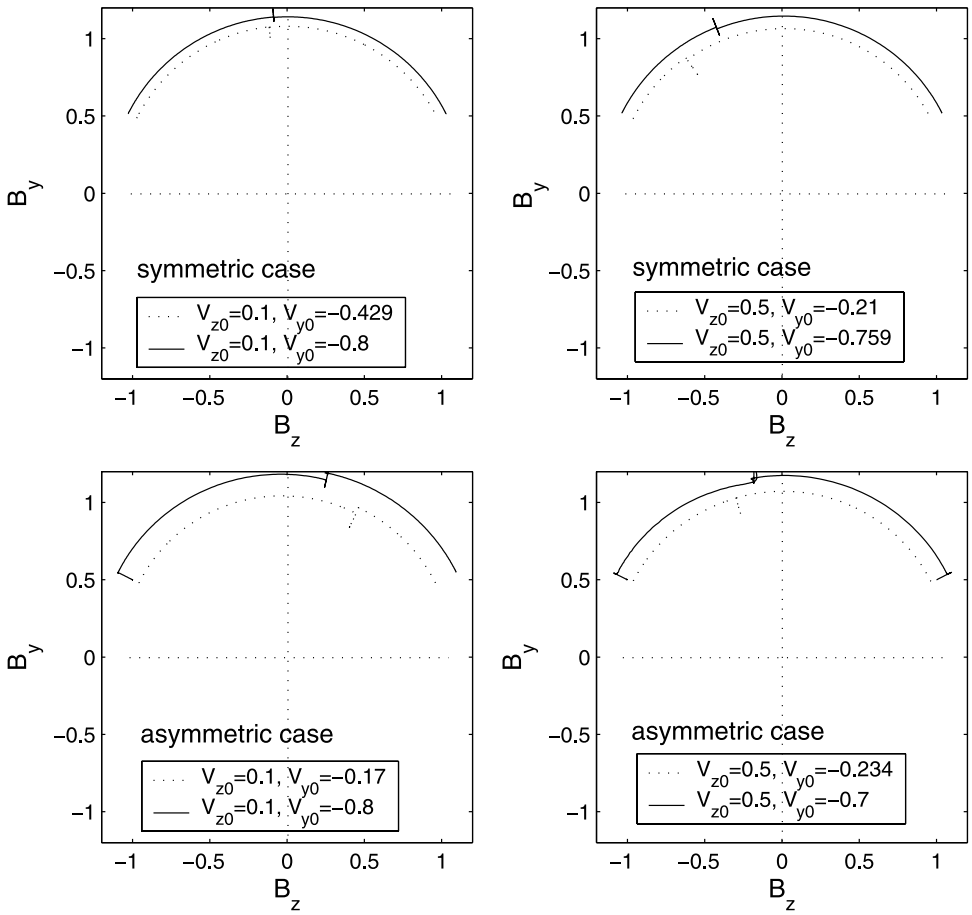

Figure 13. Magnetic field hodograms for symmetric cases (top row) and asymmetric cases (bottom row) under $V_{y0} < 0$ and $V_{z0} > 0$: there exists no reversal of the field rotation sense in either time-dependent intermediate shock when $V_{y0} < 0$.

decreases with V_{z0}, while the critical speed $V_{y0} = V'_c$ for the field reversal in TDIS′ increases with $Vz0$.

[29] On the other hand, for the case with asymmetric density, the point that marks the equal strengths, or the field rotation angles, of TDIS and TDIS′ has shifted to $V_{z0} \simeq 0.31$. At $V_{z0} = 0.31$, the curves of $V_{y0} = V_c(V_{z0})$ and $V_{y0} = V'_c(V_{z0})$ crosses at $V_c = V'_c = 0.317$. If V_{z0} is larger (smaller) than this critical value $\simeq$0.31, TDIS (TDIS′) on the left (right) is weaker than TDIS′ (TDIS) on the right (left). The value 0.31 is close to $(V_{Az2} - V_{Az1})/2$, consistent with the prediction by *Lin and Lee* [1994]. Note that all the values of V_{z0} plotted in Figure 16 are below the alfvén resonance speed $\frac{|V_{Az1}|+|V_{Az2}|}{2}$.

[30] Note that all the above cases presented in sections 3 and 4 are for $B_{y0} > 0$. If the guide field $B_{y0} < 0$, the field reversal takes place for $V_{y0} < 0$, instead of $V_{y0} > 0$. No field reversal is found for $V_{y0} > 0$, regardless of the sign of $V_{z0} = 0$. The results are similar to those for $B_{y0} > 0$, only the field rotation is toward positive B_y when the reversed rotation occurs, as discussed by *Sun et al.* [2005].

5. Summary

[31] In this paper the structure of the reconnection layer is investigated, by solving the Riemann problem associated with the decay of an initial current sheet using a resistive MHD simulation, for the effects of various finite shear flow velocities in V_y and V_z across the current layer. The simulation is carried out for a finite guide field B_{y0}.

[32] In general, two time-dependent intermediate shocks TDIS and TDIS′ may exist on the magnetosheath and magnetospheric sides of the reconnection layer, respectively. These discontinuities carry the magnetic field direction changes across the current layer. Without the shear flows, TDIS on the magnetosheath (high density) side is stronger than TDIS′ on the magnetospheric side, possessing a larger rotation angle of the tangential magnetic field. In the presence of shear flow velocities $V_{y1} = -V_{y2} = V_{y0}$ perpendicular to the antiparallel component of the magnetic field (B_z), both the weak and strong time-dependent intermediate shocks may reverse their field rotation senses if $B_{y0}V_{y0} > 0$.

[33] For guide field $B_{y0} > 0$, the reversal of the field rotation occurs when $V_{y0} > 0$, toward negative B_y, as the shear flow speed V_{y0} exceeds the following critical speeds. For $V_{y0} > V'_c$, the weak time-dependent shock TDIS′ first reverses its field rotation sense, and then at a higher critical speeds $V_{y0} > V_c$, the strong TDIS also reverses its field rotation direction. In the critical case with $V_{y0} = V'_c$, the weak TDIS′ is replaced by an Alfvén wave pulse, across which the density, pressure, and magnetic field are conserved, and the tangential magnetic field does not change the direction. In the critical cases with $V_{y0} = V_c$, the strong

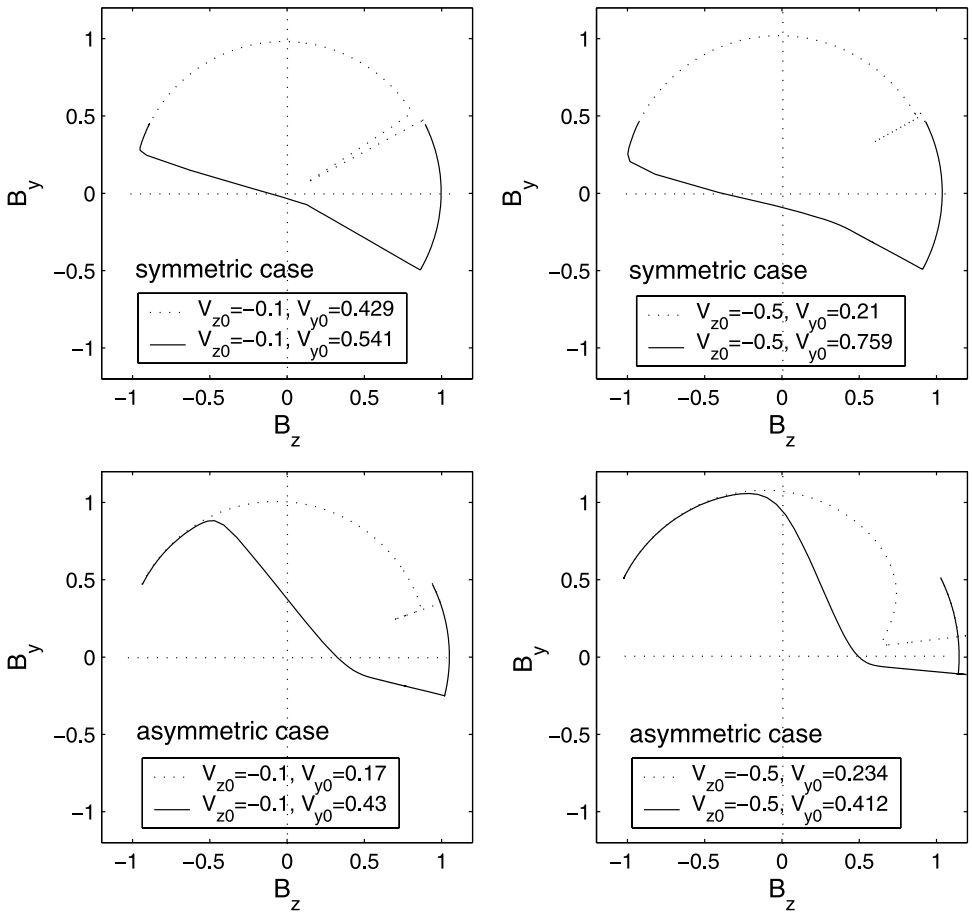

Figure 14. Magnetic field hodograms for symmetric cases (top) and asymmetric cases (bottom) with $V_{y0} > 0$ and $V_{z0} < 0$: in either time-dependent shock, the field rotation sense reverses as V_{y0} increases, but the strength of TDIS on the left is always larger than that of TDIS′ on the right when $V_{z0} < 0$.

TDIS is replaced by a steady intermediate shock, across which the tangential magnetic field changes the direction by 180°. The dependence of the critical speeds V_c and V'_c on the density ratio ρ_1/ρ_2 is calculated. Conversely, no reversal of the field rotation sense is found for $V_{y1} = -V_{y2} = V_{y0} < 0$ if $B_{y0} > 0$.

[34] If there also exists a finite shear flow component along the antiparallel magnetic field direction, i.e., $V_{z1} = -V_{z2} = V_{z0} \neq 0$, the structure of the reconnection layer and the critical velocities for the reversal of the magnetic field are greatly modified. For $V_{z0} > 0$, the TDIS′ on the magnetospheric side can become stronger than TDIS on the magnetosheath side, as obtained from earlier simulations [*Lin and Lee*, 1994]. For $V_{z0} < 0$, however, TDIS on the magnetosheath side is always stronger than TDIS′, and the strength of TDIS (TDIS′) increases (decreases) with $|V_{z0}|$. The reversal of the field rotation sense in TDIS and TDIS′ also occurs, regardless the sign of V_{z0}, as long as $V_{y0}B_{y0} > 0$. The critical speeds $V_{y0} = V_c$ and $V_{y0} = V'_c$ for the reversal of TDIS and TDIS′, respectively, vary with V_{z0}.

[35] The results shown in this paper can be applied not only to reconnections in the magnetosphere, but also to other space plasma regions and laboratory experiments [*Park et al.*, 2003] where magnetic reconnection may be accompanied by a sheared flow. In the magnetosphere, shear flows have been observed at various locations away from the subsolar region, and they may be parallel or perpendicular to the antiparallel magnetic field component, depending on the locations and the magnetic field geometries of local reconnection events. According to our investigation, the sense of the field rotation in MHD discontinuities in the reconnection layer can be different for different signs of the shear flow velocities, and the occurrence of the field reversal is only for a selected sign of V_{y0}, for a given guide field B_{y0}. The finding that various shear flows in V_y and V_z result in specifically different magnetic field structures in the reconnection layer provides useful information for the identification of reconnection signatures in space and laboratory plasmas.

[36] Finally, it should also be noted that our results obtained from the 1-D Riemann problem has its limitations. Two important remarks are made here about the multidimensional effects of shear flows in a current sheet. First, it is well known that shear flows may lead to Kelvin-Helmholtz (KH) instability. The most unstable modes of the KH instability have been found to occur when the shear flow is perpendicular to the magnetic field and/or the magnetic tension force. In the presence of a shear flow in V_y and an antiparallel field in B_z, the structure of magnetic reconnection as well as the associated waves are of three-dimensional (3-D) nature. A 3-D model is required to understand the important issues such as whether the KH

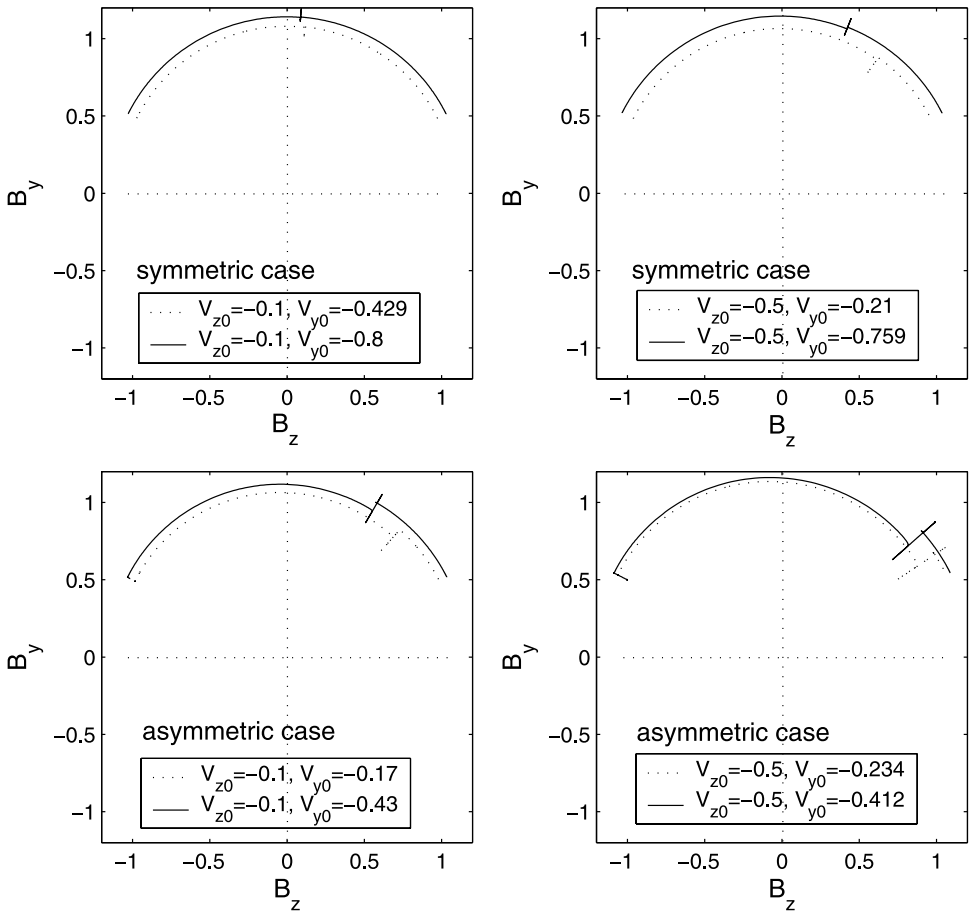

Figure 15. Magnetic field hodograms for symmetric cases (top) and asymmetric cases (bottom) with $V_{y0} < 0$ and $V_{z0} < 0$.

modes or tearing modes is dominant and if the waves of reconnection, which would propagate in the *x*-*z* plane in a 2-D current sheet, are affected by the perturbation in V_y. Second, previous studies for cases with shear flows along the antiparallel components of magnetic field have found that as the external flow speeds on both sides of the current sheet approach the local Alfvén speed (characterized by B_z), an Alfvén resonance occurs [*Wang et al.*, 1998], and the

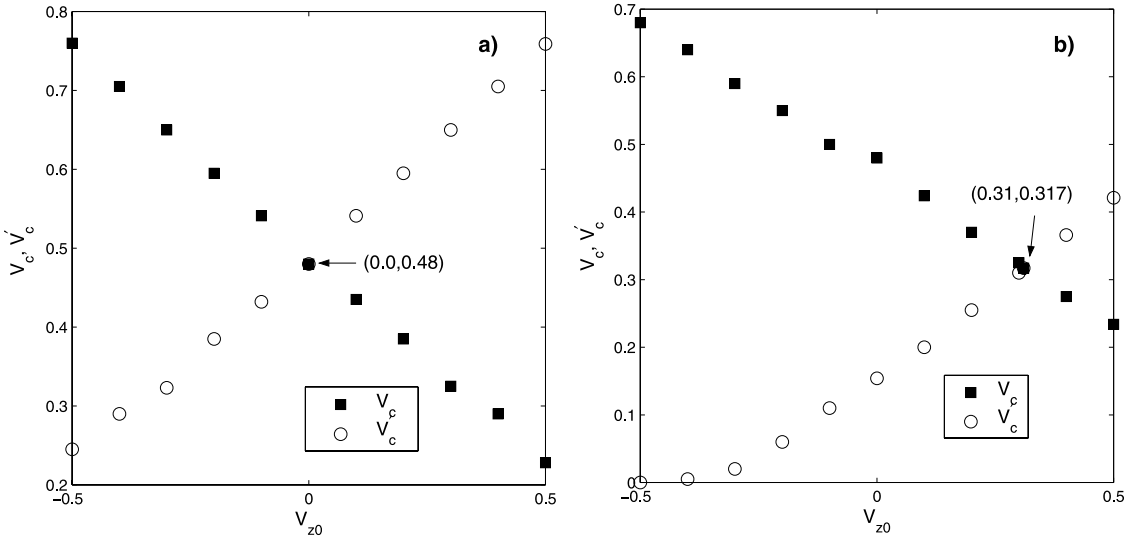

Figure 16. The critical speeds V_c and V'_c as a function of V_{z0}: (a) symmetric case with density $\rho_1 = \rho_2$ and magnetic field strength $B_1 = B_2$ and (b) asymmetric case with $\rho_1 = 10\rho_2$ and $B_1 = B_2$.

reconnection is turned off [*La Belle-Hamer et al.*, 1995]. The cases discussed here, however, are for shear flows perpendicular to B_z. In a 2-D current sheet with $\partial/\partial y = 0$, the wave vectors in the reconnection layer are mainly along z, the condition of Alfvén resonance cannot be reached. Nevertheless, the 3-D structure of reconnection, which is beyond the scope of this paper, may cause more complicated results.

[37] **Acknowledgments.** This work is supported by NSFC grants 10575018, 40390155, and 40228006 to Dalian University of Technology and NASA grant NAG5-12899 to Auburn University.

[38] Amitava Bhattacharjee thanks the reviewers for their assistance in evaluating this paper.

References

Fedorov, A., E. Budnik, H. Stenuit, T. Moreau, and J.-A. Sauvaud (2003), Antiparallel reconnection as a possible source of high- and low-latitude boundary layer, in *Earth's Low-Latitude Boundary Layer*, *Geophys. Monogr. Ser.*, vol. 133, edited by P. T. Newell and T. Onsager, p. 139, AGU, Washington, D. C.

Fusilier, S. A., K. J. Trattner, and S. M. Petrinec (2000), Cusp observations of high- and low-latitude reconnection for northward interplanetary magnetic field, *J. Geophys. Res.*, *105*, 253.

Gosling, J. T., M. F. Thomsen, S. J. Bame, and C. T. Russell (1986), Accelerated plasma flows at the near-tail magnetopause, *J. Geophys. Res.*, *91*, 3029.

Gosling, J. T., M. F. Thomsen, S. J. Bame, R. C. Elphic, and C. T. Russell (1991), Observations of reconnection of interplanetary and lobe magnetic field lines at the high-latitude magnetopause, *J. Geophys. Res.*, *96*, 14,097.

Heyn, M. F., H. K. Biernat, R. P. Rijnbeek, and V. S. Semenov (1988), The structure of reconnection layers, *J. Plasma Phys.*, *40*.

Jeffrey, A., and T. Taniuti (1964), *Nonlinear Wave Propagation*, Elsevier, New York.

La Belle-Hamer, A. L., A. Otto, and L. C. Lee (1994), Magnetic reconnection in the presence of sheared plasma flow: Intermediate shock formation, *Phys. Plasmas*, *1*, 706.

La Belle-Hamer, A. L., A. Otto, and L. C. Lee (1995), Magnetic reconnection in the presence of sheared flow and density asymmetry: Applications to the Earth's magnetopause, *J. Geophys. Res.*, *100*, 11,875.

Landau, L. D., and E. M. Lifshitz (1960), *Electrodynamics of Continous Media*, 240 pp., Elsevier, New York.

Lin, Y., and L. C. Lee (1993a), Structure of the dayside reconnection layer in resistive MHD and hybrid models, *J. Geophys. Res.*, *98*, 3919.

Lin, Y., and L. C. Lee (1993b), Structure of reconnection layers in the magnetosphere, *Space Sci. Rev.*, *65*, 59.

Lin, Y., and L. C. Lee (1994), Reconnection layer at the flank magnetopause in the presence of shear flow, *Geophys. Res. Lett.*, *21*, 855.

Lin, Y., and L. C. Lee (1999), Reconnection layers in two-dimensional magnetohydrodynamics and comparison with the one-dimensional Riemann problem, *Phys. Plasma*, *6*, 3131.

Lin, Y., L. C. Lee, and C. F. Kennel (1992), The role of intermediate shocks in magnetic reconnection, *Geophys. Res. Lett.*, *19*, 229.

Miura, A. (2002), Minimum energy state and minimum angle rotation of the magnetic field in a current sheet with sheared magnetic field, *J. Geophys. Res.*, *107*(A7), 1143, doi:10.1029/2001JA009177.

Park, W., et al. (2003), Nonlinear simulation studies of tokamaks and STs, *Nucl. Fusion*, *43*, 483.

Petschek, H. E. (1964), Magnetic field annihilation, in *AAS-NASA Symposium on the Physics of Solar Flares*, edited by W. N. Hess, *NASA Spec. Publ.*, *SP-50*, 425–439.

Phan, T. D., B. U. O. Sonnerup, and R. P. Lin (2001), Fluid and kinetics signatures of reconnection at the dawn tail magnetopause: Wind observations, *J. Geophys. Res.*, *106*, 25,489.

Sun, X. X., Y. Lin, and X. G. Wang (2005), Structure of reconnection layer with a shear flow perpendicular to the antiparallel magnetic field component, *Phys. Plasmas*, *12*, 12,305.

Wang, X., A. Bhattacharjee, Z. W. Ma, C. Ren, C. C. Hegna, and J. D. Callen (1998), Structure and dynamics of current sheets at Alfvén resonances in a differentially rotating plasma, *Phys. Plasmas*, *5*, 2291.

Wu, C. C. (1988), Effects of dissipation on rotational discontinuities, *J. Geophys. Res.*, *93*, 3969.

Wu, C. C. (1990), Formation, structure, and stability of MHD intermediate shocks, *J. Geophys. Res.*, *95*, 8149.

Wu, C. C., and C. F. Kennel (1992), Structure and evolution of time-dependent intermediate shocks, *Phys. Rev. Lett.*, *68*, 56.

Xie, H., and Y. Lin (2000), Two-dimensional hybrid simulation of the dayside reconnection layer and associated ion transport, *J. Geophys. Res.*, *105*, 25,171.

Y. Lin, Physics Department, Auburn University, 206 Allison Laboratory, Auburn, AL 36849-5311, USA. (ylin@physics.auburn.edu)

X. X. Sun and X. G. Wang, State Key Laboratory of Materials Modification by Beams, Department of Physics and College of Advanced Science and Technology, Dalian University of Technology, Dalian, China 116024. (xxsun@student.dlut.edu.cn; xgwang@dlut.edu.cn)